Eur. Phys. J. Plus (2015) **130**: 57
DOI 10.1140/epjp/i2015-15057-9

THE EUROPEAN PHYSICAL JOURNAL PLUS

Regular Article

Exact solutions for free convection flow of nanofluids with ramped wall temperature

Asma Khalid[1,3,a], Ilyas Khan[2,b], and Sharidan Shafie[3,c]

[1] Department of Mathematics, SBK Women's University, Quetta 87300, Pakistan
[2] Basic Sciences Department, College of Engineering Majmaah University, Majmaah 11952, Saudi Arabia
[3] Department of Mathematical Sciences, Faculty of Science, Universiti Teknologi Malaysia 81310 UTM Skudai, Malaysia

Received: 10 October 2014 / Revised: 31 January 2015
Published online: 1 April 2015 –

Abstract. This article aims to study the unsteady convection flow of nanofluids induced by free convection and the oscillating plate condition. The fluid is confined to the region over an infinite vertical flat plate with ramped wall temperature. Five different types of water-based nanofluids containing copper (Cu), silver (Ag), copper oxide (CuO), alumina (Al_2O_3) and titanium oxide (TiO_2) are chosen for this analysis. The Laplace transform technique is applied to obtain exact solutions of velocity and temperature for both cases of ramp and isothermal plate conditions. Ramp and isothermal solutions are compared graphically and it is found that the ramp velocity and the temperature are smaller in magnitude than isothermal velocity and temperature. Corresponding expressions for skin-friction and Nusselt number are also evaluated. The results are plotted for various physical parameters contained in the governing equations and discussed in details. Comparison with earlier results provides an excellent agreement.

1 Introduction

The convection flow arises in many physical situations such as in the food industry. Convection is divided into three main types, namely free, mixed and force. Amongst them free convection is of great significance. Apart from its several engineering applications, free convection is found in many physical phenomenons, for example, when hot surfaces, such as retorts with or without insulation, are exposed to colder ambient air. It also occurs when food is placed inside a chiller or freezer store in which circulation is not assisted by fans. Natural convection is also useful when material is placed in ovens without fans and afterwards when the cooked material is removed to cool in air. Some recent studies containing the free convection phenomenon can be found in refs. [1–5] and references therein. Besides that, the work on free convection for nanofluids when exact solutions are needed is limited.

On the other hand, the conventional heat transfer fluids such as oil, water, and ethylene glycol mixtures are poor heat transfer fluids due to their poor thermal conductivity. As the scientists believe, low thermal conductivity is one of the basic limitations in the development of energy-efficient heat transfer fluids that are required in many industrial applications. Therefore, many attempts have been made by researchers to enhance the thermal conductivity of these fluids. This work was pioneered by Choi [6], where he pointed out that an innovative new class of heat transfer fluids can be engineered by suspending metallic nanoparticles in conventional heat transfer fluids. The resulting fluids known as nanofluids are expected to exhibit high thermal conductivities compared to those of currently used heat transfer fluids. The nanoparticles used in nanofluids are made of metals (Al, Cu), carbides, metal oxides, nitrides or non-metals (graphite, carbon nano-tubes) and the base fluid is usually liquid such as water or ethylene glycol [7]. After the seminal work of Choi [6], many investigators studied nanofluids including the important work of Eastman [8,9], Das *et al.* [10, 11] and Boungiorno [12,13].

Ahmed and Pop [14] analysed the steady mixed convection boundary layer flow past a vertical flat plate embedded in a porous medium filled with nanofluid. Hamad *et al.* [15] studied the magnetic field effects on free convection flow of a nanofluid past a vertical semi-infinite flat plate followed by Hamad [16], where he obtained analytical solution

[a] e-mail: awaisiasma@gmail.com
[b] e-mail: ilyaskhanqau@yahoo.com
[c] e-mail: sharidan@utm.my

for natural convection flow of nanofluids over a linearly stretching sheet in the presence of a magnetic field. The conjugate phenomenon of heat and mass transfer of nanofluids over a moving permeable surface with convective boundary conditions has been analysed by Qasim *et al.* [17]. Few other problems on nanofluids studied through different approaches are given in some recent attempts [18–27]. All these studies are performed either using numerical or any approximate scheme. Exact solutions for nanofluids are very rare. The first exact solution for nanofluids is that obtained by Loganathan *et al.* [28]. They carried out an exact analysis to study the influence of thermal radiation on the unsteady natural convection flow of a nanofluid past an impulsively started infinite vertical plate using the Laplace transform method. After his seminal work, Turkyilmazoglu [29] observed the unsteady convection flow of some nanofluids past a moving vertical flat plate with heat transfer. The governing equations are solved for exact solutions using two types of boundary conditions, namely, prescribed uniform wall temperature (PST) and prescribed uniform heat flux (PHF).

All the above investigations are carried out under continuous and well-defined conditions for velocity and temperature at the interface of the plate. However, there exist several problems of physical interest, which may require ramped wall conditions. Taking into account this fact, several researchers investigated the problems of free convection from a vertical plate with ramped wall temperature. In the earlier studies on free convection with discontinuous wall temperature, include the work of Hayday *et al.* [30], Kelleher [31] and Kao [32].

After the seminal work of Schetz and Eichhorm [33], Chandran *et al.* [34] seem to be the first who studied the unsteady natural convection flow of a viscous fluid past a vertical plate with ramped wall temperature. By considering the fluid to be at rest all the time, they obtained exact solutions for velocity and temperature for both cases of ramped and isothermal plate conditions. Seth *et al.* [35] explored the magnetohydrodynamics (MHD) natural convection flow with radiative heat transfer past an impulsively moving plate in a porous medium with ramped wall temperature. Narahari *et al.* [36] analyzed radiation effects on the free convection flow past an impulsively started infinite vertical plate with ramped wall temperature and constant mass diffusion. The unsteady hydromagnetic radiative flow of a nanofluid past a flat plate suddenly started in motion with ramped wall temperature was examined by Nandkeolyar *et al.* [37]. MHD free convection flow in a porous medium with thermal diffusion and ramped wall temperature has been investigated by Samiulhaq *et al.* [38]. In the subsequent year, Samiulhaq *et al.* [39] extended their idea from viscous fluid to non-Newtonian second grade fluid and studied the effects of MHD and porosity on free convection flow near an infinite vertical flat plate with ramped wall temperature. Ismail *et al.* [40] studied MHD and radiation effects on natural convection flow in a porous medium past an infinite inclined plate with ramped wall temperature.

The purpose of present study is to investigate the unsteady free convection flow of nanofluids over an infinite vertically oscillating flat plate with ramped wall temperature. Four different types of water-based nanofluids, Al_2O_3, Cu, TiO_2, and Ag, are chosen for the analysis. Exact solutions for velocity and temperature are obtained for both cases of ramp and isothermal plate conditions. Expressions for skin friction and Nusselt are also evaluated. Results are plotted for physical parameters of interest and discussed. The present study is significant due to two main reasons. Its immediate application is found in those processes which are highly affected with heat enhancement concept. Secondly, exact solutions obtained here can be used to discover some hidden physical properties of widespread nanofluids. More exactly, these solutions can be used as a check of correctness for other nanofluids studies obtained via experimental, numerical or approximate schemes.

The rest of the paper is arranged as follows. The problem is formulated in sect. 2. Sections 3 and 4 include the solution of the problem. Special cases, Nusselt number and skin friction, and limiting cases are described in sects. 5, 6 and 7, respectively. Section 8 contains the plotted results and related discussion. This paper is concluded in sect. 9.

2 Mathematical formulation of the problem

Let us consider an incompressible, nanofluid of constant kinematic viscosity $\nu_{\rm nf}$ occupying a semi-finite space $y > 0$, with the y-axis in the vertical direction, bounded by an impermeable wall at $y = 0$. The half space plate is embedded in a medium saturated with water-based nanofluids. The base fluid and the nanoparticles are assumed to be in thermal equilibrium and no slip occurs between them. Initially, at time $t = 0$, both the fluid and the plate are at rest with constant temperature T_∞. At time $t = 0^+$, the plate is subjected to sinusoidal oscillations so that the x velocity on the wall is given by $\mathrm{V} = UH(t)\cos(\omega t)$ or $U\sin(\omega t)$, resulting in the induced nanofluid flow. More exactly, the plate begins to oscillate in its plane ($y = 0$) according to

$$\mathbf{V} = UH(t)\cos(\omega t)\mathrm{i}; \quad \text{or} \quad \mathbf{V} = U\sin(\omega t)\mathrm{i}; \quad t > 0, \tag{1}$$

where the constant U is the amplitude of the motion, $H(t)$ is the unit step function, $\mathbf{i}$ is the unit vector in the vertical flow direction and ω is the frequency of oscillation of the plate. At the same time $t = 0^+$, the temperature of the plate is raised or lowered to $T_\infty + (T_w - T_\infty)t/t_0$ when $t \leq t_0$, and thereafter, for $t > t_0$, is maintained at the constant temperature T_w. The velocity decays to zero and temperature approaches constant value T_∞ as $y \to \infty$. (See fig. 1.)

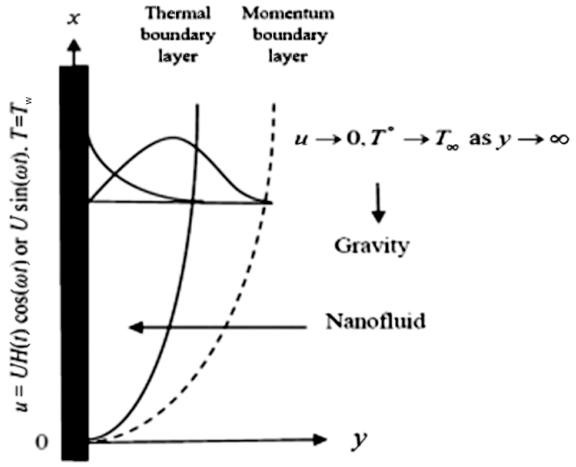

Fig. 1. Physical model and coordinate system.

Our main purpose here is to study the convection flow resulting from the buoyancy force and oscillating bounding plate with ramped wall temperature. Under these conditions along with the assumptions of usual Boussinesq approximation and that the viscous dissipation term in the energy equation is neglected, the governing equations can be written in the following form:

$$\rho_{\rm nf}\frac{\partial u}{\partial t} = \mu_{\rm nf}\frac{\partial^2 u}{\partial y^2} + g(\rho\beta)_{\rm nf}(T - T_\infty), \tag{2}$$

$$(\rho c_p)_{\rm nf}\frac{\partial T}{\partial t} = k_{\rm nf}\frac{\partial^2 T}{\partial y^2}, \tag{3}$$

subjected to the following initial and boundary conditions

$$\begin{aligned}
&u^*(y,0) = 0, \quad T^*(y,0) = T_\infty; \quad y \geq 0,\\
&u(0,t) = UH(t)\cos(\omega t) \quad \text{or} \quad U\sin(\omega t), \quad T = T_w,\\
&T^*(0,t) = T_\infty + (T_w - T_\infty)\frac{t^*}{t_0}, \quad 0 < t^* \leq t_0,\\
&T^*(0,t) = T_w, \quad t^* \geq t_0,\\
&u(y,t) \to 0, \quad T^*(y,t) \to T_\infty \quad \text{as} \quad y \to \infty \quad \text{and} \quad t^* \geq 0,
\end{aligned} \tag{4}$$

where u is the x-component of velocity, T is the temperature of nanofluid, T_w is the constant plate temperature with $T_w > T_\infty$ (temperature far away from the plate), U is the representative velocity, ω is the frequency of the oscillation at the wall, g is gravitational acceleration, $k_{\rm nf}$ is the thermal conductivity of nanofluid, $\mu_{\rm nf}$ is the dynamic viscosity of the nanofluid, $(\rho c_p)_{\rm nf}$ is the heat capacitance of the nanofluid, $\beta_{\rm nf}$ is the thermal expansion coefficient of the nanofluid. For nanofluids, the expressions of $\mu_{\rm nf}$, $\rho\beta_{\rm nf}$, $(\rho c_p)_{\rm nf}$ are given by [22]

$$\begin{aligned}
\mu_{\rm nf} &= \frac{\mu_f}{(1-\phi)^{2.5}}, \quad \rho_{\rm nf} = (1-\phi)\rho_{\rm f} + \phi\rho_{\rm s},\\
\frac{k_{\rm nf}}{k_{\rm f}} &= \frac{(k_{\rm s} + 2k_{\rm f}) - 2\phi(k_{\rm f} - k_{\rm s})}{(k_{\rm s} + 2k_{\rm f}) + \phi(k_{\rm f} - k_{\rm s})},\\
(\rho c_p)_{\rm nf} &= (1-\phi)(\rho c_p)_{\rm f} + \phi(\rho c_p)_{\rm s},
\end{aligned} \tag{5}$$

where ϕ is the nanoparticle volume fraction, $\rho_{\rm f}$ is the density of the base fluid, $\rho_{\rm s}$ is the density of the solid particle, c_p is the specific heat at constant pressure. As pointed out by Turkyilmazoglu [27], the expressions in eq. (5) are restricted to spherical nanoparticles. For other shapes of nanoparticles with different thermal conductivity and dynamic viscosity, the reader is referred to table 1 [22].

For dimensionless analysis, we introduce the non-dimensional quantities defined by

$$\begin{aligned}
&u = \frac{u^*}{U}, \qquad y = \frac{y^*}{\sqrt{\nu t_0}}, \qquad t = \frac{t^*}{t_0},\\
&T = \frac{T^* - T_\infty}{T_w - T_\infty}, \qquad t_0 = \left(\frac{\sqrt{\nu}}{g\beta(T_w^* - T_\infty^*)}\right)^{2/3}.
\end{aligned} \tag{6}$$

Table 1. Thermophysical properties of water and nanoparticles [22].

	ρ (Kg m^{-3})	c_p (Kg^{-1}K^{-1})	k (Wm^{-1}K^{-1})	$\beta \times 10^{-5}$ (K^{-1})
H_2O	997.1	4179	0.613	21
Al_2O_3	3970	765	40	0.85
Cu	8933	385	401	1.67
TiO_2	4250	686.2	8.9528	0.9
Ag	10500	235	429	1.89

The dimensionless problem is, therefore, given as

$$\frac{\partial u}{\partial t} = \frac{1}{\mathrm{Re}}\frac{\partial^2 u}{\partial y^2} + \phi_1 Gr\, T, \tag{7}$$

$$\mathrm{Pr}\,\frac{\partial T}{\partial t} = \frac{1}{\phi_2}\frac{\partial^2 T}{\partial y^2}, \tag{8}$$

$$u(y,0) = 0, \quad T(y,0) = T_\infty; \quad y \geq 0,$$

$$u(0,t) = H(t)\cos(\omega t) \quad \text{or} \quad \sin(\omega t), \quad T = T_w,$$

$$T(0,t) = \begin{cases} t, & 0 < t \leq 1 \\ 1, & t > 1 \end{cases} = tH(t) - (t-1)H(t-1)$$

$$u(y,t) \to 0, \quad T(y,t) \to 0 \quad \text{as} \quad y \to \infty \quad \text{and} \quad t \geq 0, \tag{9}$$

where $\mathrm{Re} = (1-\phi)^{2.5}\{(1-\phi) + \phi(\frac{\rho_s}{\rho_f})\}$ is the Reynolds number, $\mathrm{Pr} = \frac{(\mu c_p)_f}{k_f}$ is the Prandtl number, $Gr = \frac{g\beta(T_w - T_\infty)t_0}{u}$ is the Grashof number and $\phi_1 = \{\frac{(1-\phi)\rho_f + \phi\rho_s(\frac{\beta_s}{\beta_f})}{\rho_{nf}}\}$, $\phi_2 = \{(1-\phi) + \phi\frac{(\rho c_p)_s}{(\rho c_p)_f}\}$ are functions depending upon the thermophysical properties of the base fluid and nanoparticles.

3 Exact solutions

In order to find exact solutions of the system of eqs. (7) and (8), we use the Laplace transform technique. Thus by taking the Laplace transforms of eqs. (7) and (8), using initial and boundary conditions (9), we get the following solutions in the transformed (y, q) plane:

$$\overline{u}(y,q) = \left[\frac{q}{q^2+\omega^2} + a\frac{(1-e^{-q})}{q^3}\right] e^{-y\sqrt{\mathrm{Re}\,q}} - a\frac{(1-e^{-q})}{q^3}e^{-y\sqrt{bq}}, \tag{10}$$

$$\overline{T}(y,q) = \left(\frac{1-e^{-q}}{q^2}\right) e^{-y\sqrt{bq}}, \tag{11}$$

where

$$a = \frac{\mathrm{Re}\,\phi_1 Gr}{\mathrm{Pr} - 1} \quad \text{and} \quad b = \phi_2\,\mathrm{Pr}\,.$$

The inverse Laplace transforms of eqs. (10) and (11) are obtained as follows:

$$T_{\mathrm{ramp}}(y,t) = T_1(y,t) - T_1(y,t-1)H(t-1), \tag{12}$$

$$T_1(y,t) = \left[\left(t + \frac{by^2}{2}\right)\mathrm{erf}\,c\left(\frac{y}{2}\sqrt{\frac{b}{t}}\right) - y\sqrt{b}\sqrt{\frac{t}{\pi}}e^{-\frac{by^2}{4t}}\right], \tag{13}$$

$$u_{c(\mathrm{ramp})}(y,t) = u_1(y,t) + u_2(y,t) + [u_3(y,t) - u_3(y,t-1)H(t-1)] - [u_4(y,t) - u_4(y,t-1)H(t-1)], \tag{14}$$

$$u_{s(\mathrm{ramp})}(y,t) = -iu_1(y,t) - iu_2(y,t) + [u_3(y,t) - u_3(y,t-1)H(t-1)] - [u_4(y,t) - u_4(y,t-1)H(t-1)], \tag{15}$$

where the subscripts c and s correspond to cosine and sine oscillations of the plate, respectively, the component velocities $u_i(i = 1, \ldots, 4)$ are defined as

$$u_1(y,t) = \frac{H(t)}{4} e^{-i\omega t} \left[e^{-y\sqrt{-\mathrm{Re}\, i\omega}} \mathrm{erf}\, c \left(\frac{y}{2}\sqrt{\frac{\mathrm{Re}}{t}} - \sqrt{-i\omega t} \right) + e^{y\sqrt{-\mathrm{Re}\, i\omega}} \mathrm{erf}\, c \left(\frac{y}{2}\sqrt{\frac{\mathrm{Re}}{t}} + \sqrt{-i\omega t} \right) \right], \tag{16}$$

$$u_2(y,t) = \frac{H(t)}{4} e^{i\omega t} \left[e^{-y\sqrt{\mathrm{Re}\, i\omega}} \mathrm{erf}\, c \left(\frac{y}{2}\sqrt{\frac{\mathrm{Re}}{t}} - \sqrt{i\omega t} \right) + e^{y\sqrt{\mathrm{Re}\, i\omega}} \mathrm{erf}\, c \left(\frac{y}{2}\sqrt{\frac{\mathrm{Re}}{t}} + \sqrt{i\omega t} \right) \right], \tag{17}$$

$$u_3(y,t) = \frac{a}{2} \left[\left(\left(\frac{\mathrm{Re}^2 y^4}{12} + \mathrm{Re}\, y^2 t + t^2 \right) \mathrm{erf}\, c \left(\frac{y}{2}\sqrt{\frac{\mathrm{Re}}{t}} \right) - \frac{y\sqrt{\mathrm{Re}}}{6}\sqrt{\frac{t}{\pi}} \left(\frac{\mathrm{Re}\, y^2 + 5t}{2} \right) e^{-\frac{\mathrm{Re}\, y^2}{4t}} \right) \right], \tag{18}$$

$$u_4(y,t) = \frac{a}{2} \left[\left(\left(\frac{b^2 y^4}{12} + b y^2 t + t^2 \right) \mathrm{erf}\, c \left(\frac{y}{2}\sqrt{\frac{b}{t}} \right) - \frac{\sqrt{b} y}{6}\sqrt{\frac{t}{\pi}} \left(\frac{b y^2 + 5t}{2} \right) e^{-\frac{b y^2}{4t}} \right) \right]. \tag{19}$$

4 Solution for isothermal plate

It is important to note that solutions (12), (14) and (15) are obtained for velocity and temperature when the oscillating plate admits the ramped wall condition. In order to highlight the effects of ramped temperature of the plate on the fluid flow, it is worthwhile to compare such a flow with the one near a moving plate with uniform temperature. Taking into accounts the constraints imposed on the fluid motion in sect. 2, the solutions for the fluid temperature and velocity for free convection flow near an oscillating plate with isothermal condition are obtained, and presented in the following forms:

$$T_{\mathrm{iso}}(y,t) = T_2(y,t), \tag{20}$$

$$T_2(y,t) = \mathrm{erfc} \left(\frac{y}{2}\sqrt{\frac{b}{t}} \right),$$

$$u_{c(\mathrm{iso})}(y,t) = u_1(y,t) + u_2(y,t) + u_5(y,t) - u_6(y,t), \tag{21}$$

$$u_{s(\mathrm{iso})}(y,t) = -iu_1(y,t) - iu_2(y,t) + u_5(y,t) - u_6(y,t), \tag{22}$$

$$u_5(y,t) = a \left[\left(t + \frac{\mathrm{Re}\, y^2}{2} \right) \mathrm{erf}\, c \left(\frac{y}{2}\sqrt{\frac{\mathrm{Re}}{t}} \right) - y\sqrt{\mathrm{Re}}\sqrt{\frac{t}{\pi}} e^{-\frac{\mathrm{Re}\, y^2}{4t}} \right],$$

$$u_6(y,t) = a \left[\left(t + \frac{b y^2}{2} \right) \mathrm{erf}\, c \left(\frac{y}{2}\sqrt{\frac{b}{t}} \right) - y\sqrt{b}\sqrt{\frac{t}{\pi}} e^{-\frac{b y^2}{4t}} \right].$$

5 Special cases

We can see that the solution for the velocity given by eqs. (14), (15), (21) and (22) are not valid for fluid with Prandtl number Pr = 1. On the other hand, the Prandtl number measures the ratio of viscous diffusion rate to thermal diffusion rate and is of great physical significance. The Prandlt number, as unity, physically corresponds to the case when thermal and momentum boundary layer thicknesses are of the same order of magnitude. It is easy to show that the temperature solution $T(y,t)$ is similar to eq. (12) when we replace Pr = 1. However, the solution of velocity has to be derived again starting from eq. (7) using conditions (9). Thus the corresponding solutions for the cosine and sine oscillations of the plate when Pr = 1 are given by

$$u_{c(\mathrm{ramp})}(y,t) = u_1(y,t) + u_2(y,t) + u_0(y,t) - u_0(y,t-1)H(t-1), \tag{23}$$

$$u_{s(\mathrm{ramp})}(y,t) = -iu_1(y,t) - iu_2(y,t) + u_0(y,t) - u_0(y,t-1)H(t-1), \tag{24}$$

with

$$u_0(y,t) = \frac{Gr\sqrt{\phi_2} y}{2} \left[2\sqrt{\frac{t}{\pi}} e^{-\frac{\phi_2 y^2}{4t}} - \sqrt{\phi_2} y \mathrm{erf}\, c \left(\frac{\sqrt{\phi_2} y}{2\sqrt{t}} \right) \right]. \tag{25}$$

Following a similar procedure, the solutions obtained for isothermal plate conditions when $\mathrm{Pr} = 1$, are given by

$$u_{c(\mathrm{iso})}(y,t) = u_1(y,t) + u_2(y,t) + u_0(y,t), \tag{26}$$

$$u_{s(\mathrm{iso})}(y,t) = -iu_1(y,t) - iu_2(y,t) + u_0(y,t). \tag{27}$$

6 Nusselt number and skin friction

The expressions of the Nusselt number and skin friction for ramp and isothermal conditions are determined from eqs. (12), (20), (14), (15), (26) and (27) given by

$$\mathrm{Nu} = \left.\frac{\partial T}{\partial y}\right|_{y=0},$$

$$\mathrm{Nu}_{\mathrm{iso}} = \sqrt{\frac{b}{\pi t}}, \tag{28}$$

$$\mathrm{Nu}_{\mathrm{ramp}} = -\mu[Nu_1(y,t) - Nu_1(y,t-1)H(t-1)], \tag{29}$$

where

$$\mathrm{N}_1(t) = \frac{1}{2}[\mathrm{erfc}\sqrt{bt} - \mathrm{erf}\sqrt{b(t-1)}H(t-1)],$$

$$\tau = \left.\frac{\partial u}{\partial y}\right|_{y=0},$$

$$\tau_{\mathrm{iso}} = \frac{1}{2\sqrt{\pi}}\left[e^{-it\omega}\left[-H\sqrt{\mathrm{Re}}\sqrt{\pi}\sqrt{-\mathrm{Re}\,i\omega}\,\mathrm{erf}(\sqrt{-it\omega}) - \left[2\left\{H\sqrt{\mathrm{Re}}\sqrt{\frac{1}{t}} + a\left(\sqrt{t} - \left(-1+\sqrt{b}\right)\sqrt{t}\right.\right.\right.\right.\right.$$
$$\left.\left.\left.\left.\left. - \sqrt{\frac{b}{t}}t\right)\right]\right\} + e^{-it\omega}H\sqrt{\mathrm{Re}}\sqrt{\pi}\sqrt{\mathrm{Re}\,i\omega}\mathrm{erf}(\sqrt{it\omega})\right]\right], \tag{30}$$

$$\tau_{\mathrm{ramp}}(y,t) = -\mu[\tau_1(y,t) - \tau_1(y,t-1)H(t-1)], \tag{31}$$

$$\tau_1(y,t) = \frac{1}{12\sqrt{\pi}\sqrt{t}}e^{-i\omega t}\left[-6H\sqrt{\mathrm{Re}}e^{i\omega t} + e^{i\omega t}\left[-6H\sqrt{\mathrm{Re}} + a\left\{5\sqrt{b} - \sqrt{\mathrm{Re}}\left(5 + 6\sqrt{\frac{1}{t}}\right)\sqrt{t}\right.\right.\right.$$
$$\left.\left.\left. + 6\sqrt{\frac{b}{t}}\sqrt{t}\right\}t^2\right] - 6H\sqrt{\pi}\sqrt{t}\left\{\sqrt{-\mathrm{Re}\,i\omega}\,\mathrm{erf}\left(\sqrt{-i\omega}\right) + e^{t(i\omega+i\omega)}\sqrt{\mathrm{Re}\,i\omega}\,\mathrm{erf}\left[\sqrt{it\omega}\right]\right\}\right]. \tag{32}$$

7 Limiting cases

In order to underline the theoretical value of the general solutions (14), (15) and (13) for velocity, as well as to gain physical insight of the flow regime, we consider some limiting cases whose technical relevance is well known in the literature.

7.1 Solutions for Stokes' first problem

In this case, the flow in the fluid is induced due to impulsive motion of the plate. The velocity condition at infinity and temperature conditions are same. The temperature solutions are independent of oscillation. Thus by taking $\omega = 0$ (which physically corresponds to Stokes' first problem), into eq. (14), for ramped velocity and eqs. (21) for isothermal

velocity, we obtain

$$u_{(\mathrm{ramp})}(y,t) = H(t)\left[\operatorname{erf} c\left(\frac{y\sqrt{\mathrm{Re}}}{2\sqrt{t}}\right)\right] + \frac{a}{2}\left[\left(t^2 + \mathrm{Re}\, ty^2 + \frac{\mathrm{Re}^2 y^4}{12}\right)\operatorname{erfc}\left(\frac{y\sqrt{\mathrm{Re}}}{2\sqrt{t}}\right) - \frac{(10t + \mathrm{Re}\, y^2)\sqrt{\mathrm{Re}}y\sqrt{t}e^{-\frac{\mathrm{Re}\, y^2}{4t}}}{12\sqrt{\pi}}\right] - \frac{a}{2}\left[\left(t^2 + bty^2 + \frac{b^2y^4}{12}\right)\operatorname{erfc}\left(\frac{y\sqrt{b}}{2\sqrt{t}}\right) - \frac{(10t + by^2)y\sqrt{b}\sqrt{t}e^{-\frac{by^2}{4t}}}{12\sqrt{\pi}}\right], \tag{33}$$

$$u_{(\mathrm{iso})}(y,t) = H(t)\left[\operatorname{erf} c\left(\frac{y\sqrt{\mathrm{Re}}}{2\sqrt{t}}\right)\right] + a\left[\left(t + \frac{\mathrm{Re}\, y^2}{2}\right)\operatorname{erfc}\left(\frac{y\sqrt{\mathrm{Re}}}{2\sqrt{t}}\right) - \frac{y\sqrt{\mathrm{Re}}\sqrt{t}e^{-\frac{\mathrm{Re}\, y^2}{4t}}}{2\sqrt{\pi}}\right] - a\left[\left(t + \frac{by^2}{2}\right)\operatorname{erfc}\left(\frac{y\sqrt{b}}{2\sqrt{t}}\right) - \frac{y\sqrt{b}\sqrt{t}e^{-\frac{by^2}{4t}}}{2\sqrt{\pi}}\right]. \tag{34}$$

It is important to note that eqs. (14) and (12) together with (21) and (20) are found to be identical to those obtained by Nandkeolyaret *et al.* [37], eqs. (12) and (13), and eqs.(15) and (16), respectively, when $N = 0$ (absence of thermal radiation), $M = 0$ (absence of MHD) and $1/K_1 = 0$ (absence of porosity). Hence, this verifies the correctness of the present work.

7.2 Solutions for Newtonian fluids

Here, if we want to study pure viscous fluid without incorporating the nanoparticles, we need to replace the thermal and mechanical parameters of nanofluid with those of viscous fluid in the obtained solutions (12), (14) and (20), (21). Thus, the resulting solutions will be independent of the influence of nanoparticles. These solutions will correspond to the pure convection problem when the bounding plate is at rest at all the times. They will be identical to those obtained by Chandran *et al.* [34], see eqs. (11), (12), (19) and (20).

7.3 Solution in the absence of mechanical effects

In this case, we consider the flow situation when the infinite plate is kept at rest all the times. More exactly, the wall velocity of the fluid is zero for each real value of t and thus the mechanical component of velocity identically vanishes. Consequently, the velocity of the fluid $u(y,t)$ reduces to its thermal components for both ramp and isothermal velocities. Its ramp and isothermal temperatures as well as the surface heat transfer rate are given by the same equalities. However, the skin friction will be changed correspondingly.

7.4 Solution in the absence of thermal effects

In this last case, we assume that the flow is induced only due to bounding plate and the corresponding buoyancy forces are zero equivalently it shows the absence of free convection ($Gr = 0$) due to the differences in the temperature gradient. This shows that the thermal parts of velocities in eqs. (14), (15), (21) and (22) are zero. Hence, the flow is governed only by the corresponding mechanical parts given by

$$u_{(\mathrm{ramp})}(y,t) = u_{(\mathrm{iso})}(y,t) = u_1(y,t) + u_2(y,t). \tag{35}$$

8 Numerical computation, results and discussion

This section includes the numerical computations of the obtained exact solutions. In order to highlight the effects of different physical parameters of nanofluid on velocity, temperature, Nusselt number and skin friction several graphs are plotted and tables are constructed. Water, H_2O, is taken as base fluid. Five different types of nano particles namely copper (Cu), silver (Ag), copper oxide (CuO), alumina (Al_2O_3) and titanium oxide (TiO_2) are added to water for making it as water-based nanofluids. Graphs are plotted and compared for both ramped and isothermal velocity and temperature. In fig. 2, velocity distribution $u(y,t)$ is plotted for two different values of time $t = 0.6$ and 1.5 for copper

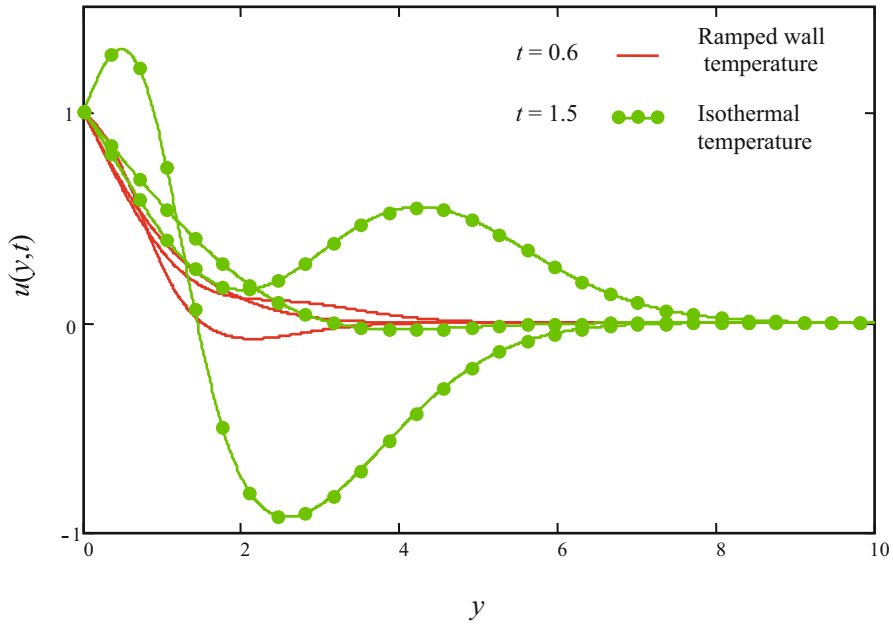

Fig. 2. The velocity profiles of copper water nanofluid of ramped wall temperature and isothermal boundary conditions for different values of Pr.

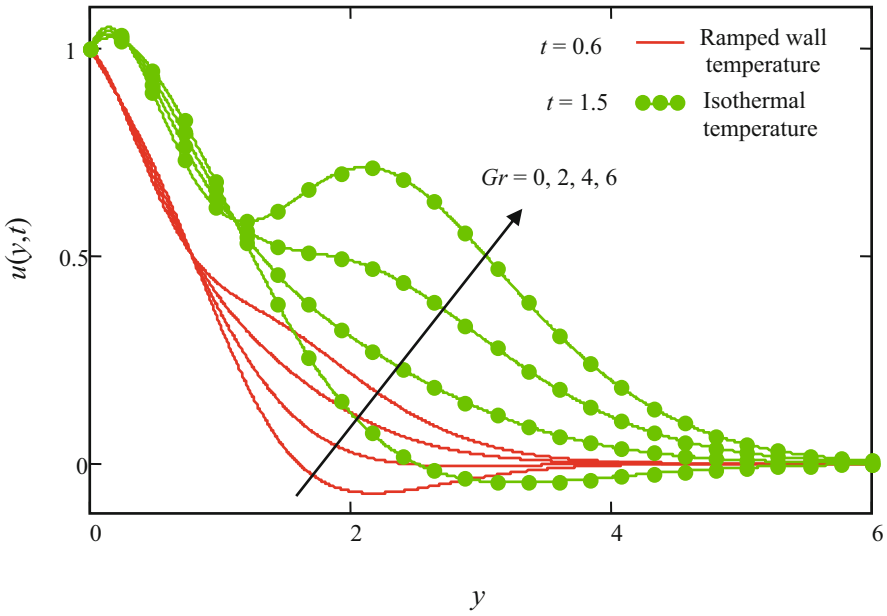

Fig. 3. Velocity profiles of Al_2O_3 water-based nanofluid for different values of Gr.

water nanofluid. The time $t = 0.6$ corresponds to the ramp velocity and $t = 1.5$ is used for isothermal plate velocity given by eqs. (14) and (21), respectively. Three different values of the Prandtl number Pr = 0.71, Pr = 1, Pr = 7 are chosen. As suggested by Loganathan *et al.* [28], the nanoparticle volume fraction is considered in the range of $0 \leq \phi \leq 0.04$, because sedimentation takes place when the nanoparticle volume fraction exceeds 8%. Furthermore, in this study, we have considered spherical nanoparticles with thermal conductivity and dynamic viscosity as shown in table 1. This choice is based on existing studies [28] and [29]. One may chose another type of nanoparticles from table 1. As we can see from the solutions that analytical results are obtained from both cosine and sine oscillations whereas the graphical results are plotted only for the cosine parts of velocity.

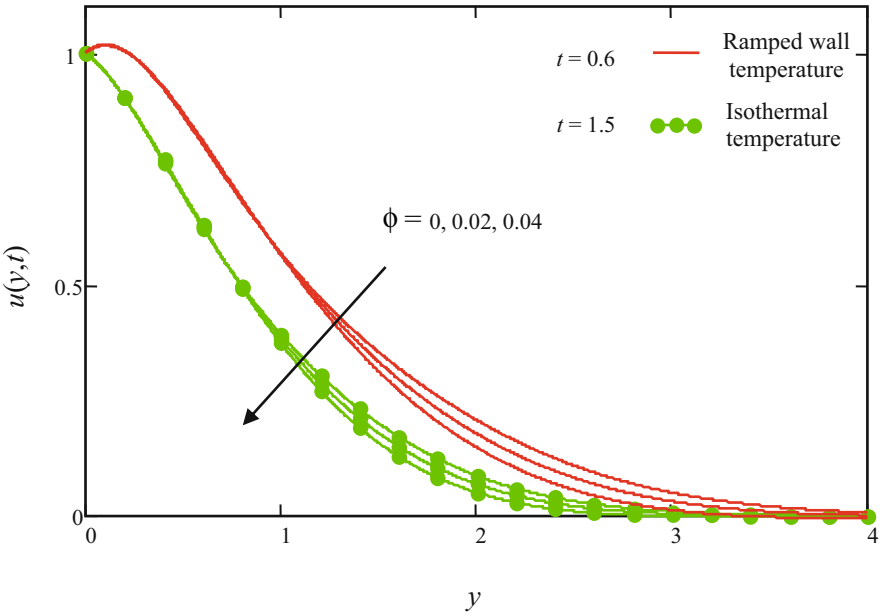

Fig. 4. Effect of nanoparticle volume fraction ϕ on the velocity profiles.

Figure 2 shows the variation in the Prandtl number for both ramped and isothermal velocities. The Prandtl number for ramped velocity as well as for isothermal velocity is takes as 0.71, 1 and 7. It is found that ramped velocity is smaller compared to isothermal velocity. This comparison is in excellent agreement with published results in literature including Chandran *et al.* [34], Sami *et al.* [39] and Nandkeolyar *et al.* [37]. However, the fluctuation in isothermal velocity is more than ramp velocity and converges faster. Further velocity in both cases first increases and then decreases. However, the variations in case of isothermal velocity are much, compared to ramped velocity. The influence of Grashof number Gr on ramped velocity (eq. (14)) and isothermal velocity (eq. (21)) for aluminium oxide nanofluid are shown in fig. 3. On the other hand, the Grashof number Gr is a dimensionless number which approximates the ratio of the buoyancy to viscous force acting on a fluid. In this figure $Gr = 0$ corresponds to the absence of free convection, while $Gr > 0$ represents the cooling problem. Here again for ramped velocity t is chosen less than unity, whereas for isothermal cases t is taken greater than 1. As in fig. 2, ramped velocity comes down than isothermal velocity. More exactly, when $Gr = 0$, physically corresponds to the absence of free convection, velocity is minimum for both ramped and isothermal cases and increases for positive values of Gr. For natural convection flow over a vertical plate, we can take $0 < Gr < 10^8$. However, in the present analysis we have taken $Gr = 2$ and 4. For Gr values bigger than this range the boundary layer becomes turbulent. This figure also shows the comparison of the absence and presence of free convection.

Figure 4 illustrates the effects of nanoparticle volume fraction ϕ on the velocity profiles for copper water nanofluid $0 \leq \phi \leq 0.04$. It is observed that as the nanoparticle volume fraction increases, the velocity of the nanofluid decreases due to increase in viscosity. This figure also shows the comparison of base fluid (water) and copper-based nanofluid. Both ramped and isothermal velocities of base fluid take minimum values compared to copper-based nanofluid. Physically, this is due to the reason that an increase in nanoparticle volume fraction leads to a decrease in the thermal conductivity of the nanofluid, hence the thickness of the thermal boundary layer decreases and viscosity increases, and finally velocity decreases. It is further inferred from this figure that changes in nanoparticle volume fraction leads to changes in temperature and then velocity which, in turn, shows the importance of nanofluids in the processes involving heating and cooling. Similarly to the previous figures, this figure also shows the comparison of ramped and isothermal velocities. The behavior is found to be identical. When $\phi = 0$, the partial differential equations (2) and (3) governing the current flow reduces to the partial differential equations to a base fluid. Further, to the case of $\phi = 0$, if the oscillating plate is kept at static position for all the times, then the resulting equations and conditions will give the same problem done by Chandran *et al.* [34].

Comparison of velocity profiles of ramped wall temperature and isothermal boundary conditions for different nanofluids, when $\mathrm{Pr} = 6.2$, $\phi = 0.04$, $Gr = 2$ is shown in fig. 5. This figure shows that Al_2O_3 water nanofluids has highest velocity followed by TiO_2, copper, and silver Ag. Variation in ramped velocity is negligible for $y < 1.8$ and $y > 4.8$. Isothermal velocity, on the other hand, shows oscillatory behavior. Figure 6 is prepared to show the

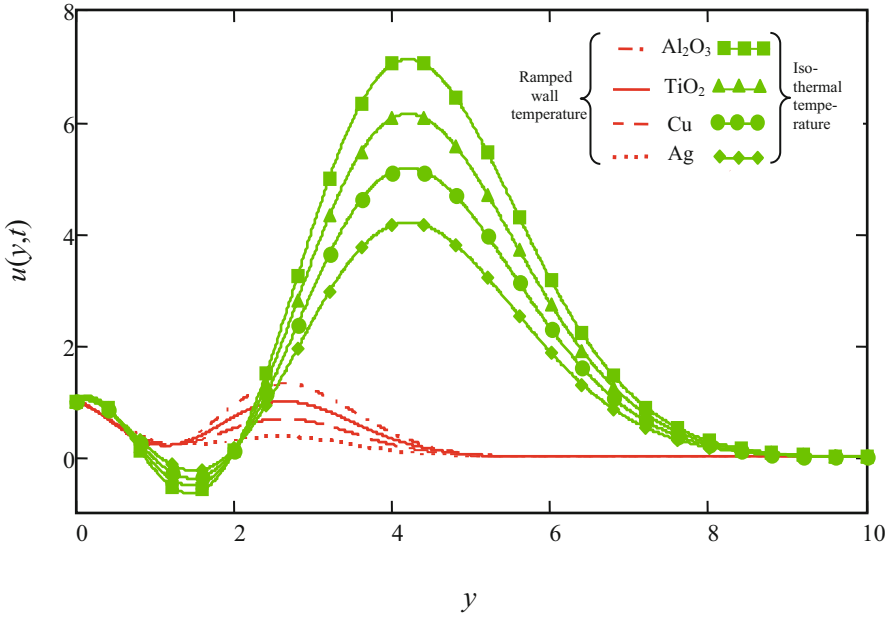

Fig. 5. Comparison of velocity profiles of ramped wall temperature and isothermal boundary conditions for different nanofluids, when Pr = 6.2, $\phi = 0.04$, $Gr = 2$.

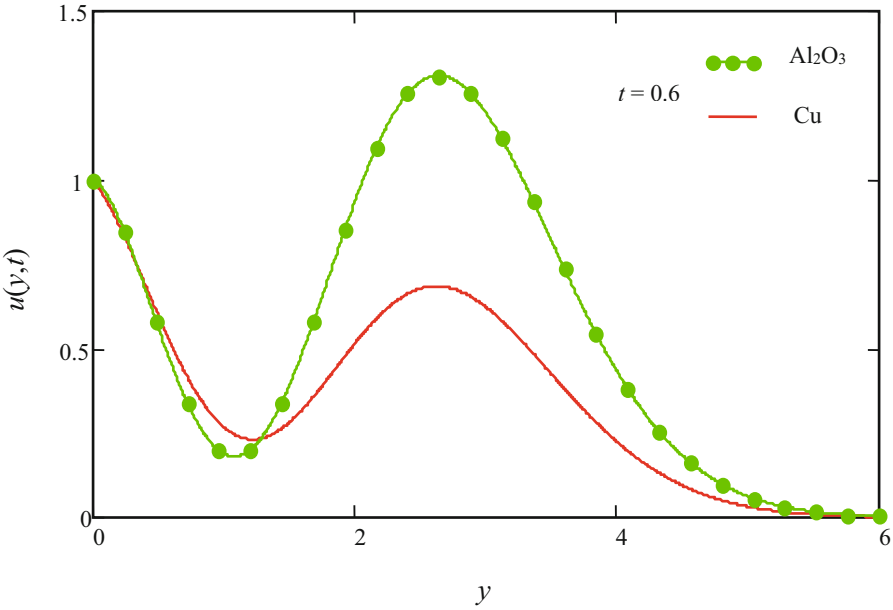

Fig. 6. Comparison of velocity profiles of Al_2O_3 and Cu for ramped wall temperature, when Pr = 6.2, $\phi = 0.04$, $Gr = 2$.

comparison for the two models of Al_2O_3 and Cu for ramped wall temperature at the same time $t = 0.6$. It is found that copper-based nanofluid velocity is more than alumina-based nanofluid near the plate. However, as the distance increases from the plate, this behaviour reverses. The presence of the nanoparticles in the fluids increases appreciably the effective thermal conductivity of the fluid and consequently enhances the heat transfer characteristics. The heat transfer near the plate is higher compared to away from the plate. The Cu nanoparticles have high values of thermal diffusivity. Therefore, velocity of the fluid with Cu nanoparticles near the plate is higher compared to the fluid with Al_2O_3. However, away from the plate this behaviour changes due to change in temperature.

Figure 7 depicts the effects of the Prandtl number on temperature profiles for copper water nanofluids for both ramped and isothermal wall temperatures. It is observed that the increasing values of Pr, it results in a decrease of the thermal boundary layer which causes the temperature to decrease. Physically, this behaviour is meaningful due to the fact that the Prandtl number increases either by increasing the size of the nanoparticle or by the viscosity of the base fluid and hence the temperature decreases. Moreover, with increasing viscosity of the base fluid, the thermal

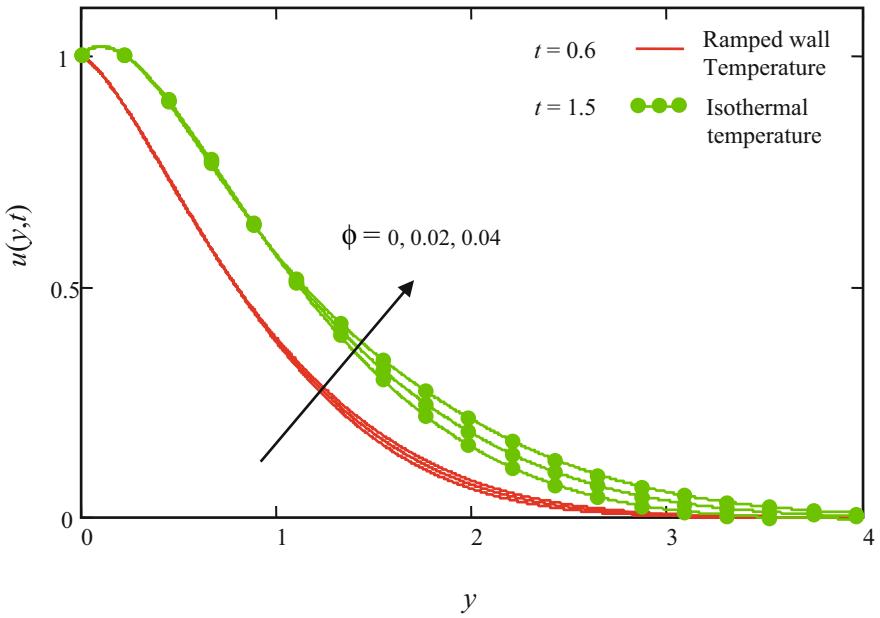

Fig. 7. Effect of nanoparticle volume fraction ϕ on the temperature of copper water nanofluid.

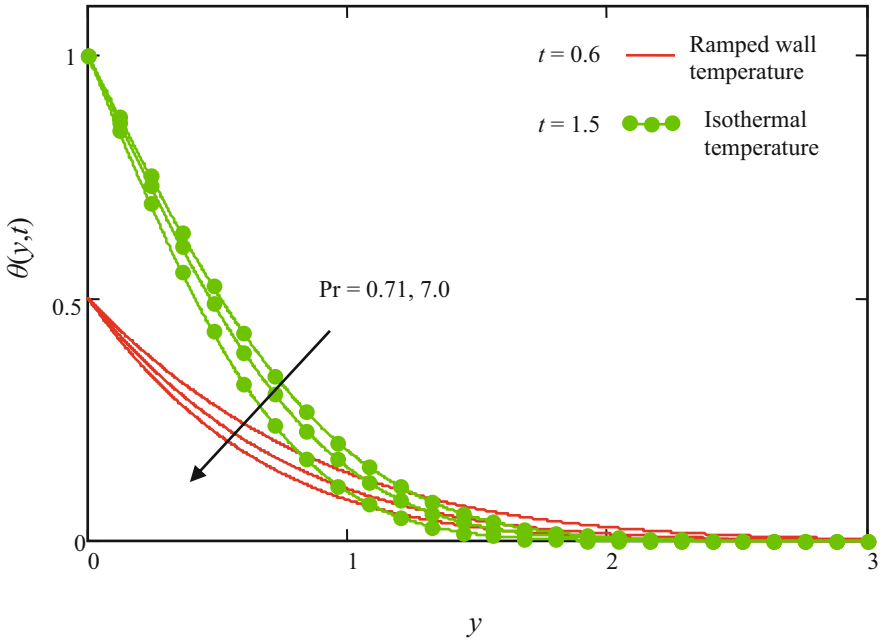

Fig. 8. Temperature profiles for ramped temperature and isothermal boundary conditions.

boundary layer thickness decreases and the heat transfer is found to be smaller for large values of Pr. A common behavior of velocity from all these graphs is noticed that the velocity of the nanofluid is maximum near the plate and decreases away from the plate. This physical behavior of velocity is in good agreement with imposed boundary conditions. Figure 8 discusses the temperature distributions of different types of nanofluids. This figure shows that the silver water nanofluid has the highest temperature distribution compared to copper, TiO_2 and Al_2O_3 water nanofluids.

Now in order to check the accuracy of the present results, the temperature and velocity profiles of the present study are compared with existing results in literature by Nandkeolyar *et al.* [37]. This comparison is shown in fig. 9. An excellent agreement is observed. The effects of Prandtl number Pr, Grashof number Gr, phase angle ωt and dimensionless time t, on skin friction and Nusselt number corresponding to isothermal and ramped velocities are studied in tables 2, 3, 4 and 5. The bold number in each table shows the variation of that parameter. An increase in

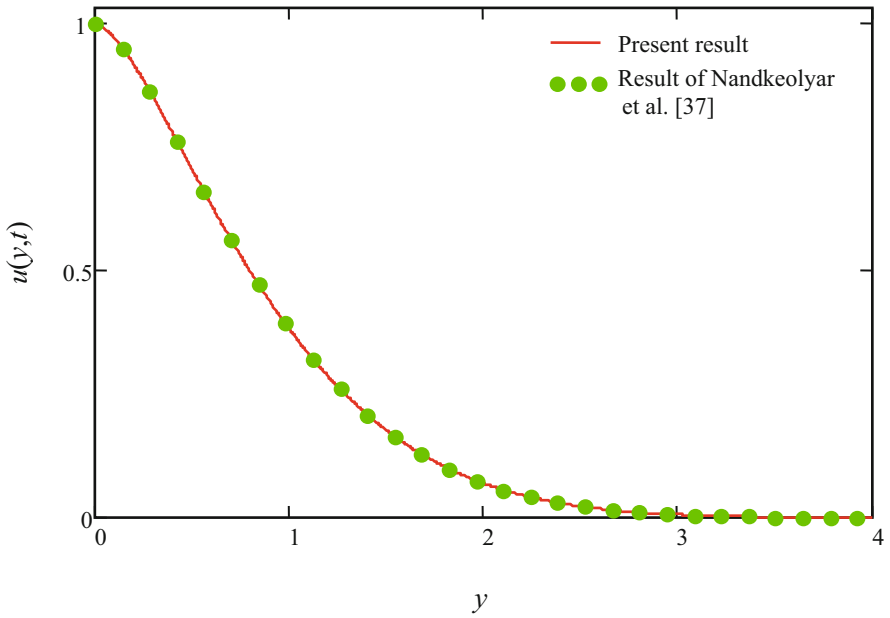

Fig. 9. Comparison of the present result [see eq. (24), when $\omega = 0$] with that obtained by Nandkeolyar *et al.* [37] (see eq. (13), when $M = N = \frac{1}{K_1} = 0$).

Table 2. Skin friction variations for ramped wall temperature.

Pr	Gr	ωt	t	τ_{ramp}
0.71	2	$\pi/4$	0.6	0.257239
7.0	2	$\pi/4$	0.6	0.386272
0.71	**4**	$\pi/4$	0.6	0.264543
0.71	2	$\boldsymbol{\pi/2}$	0.6	0.310681
0.71	2	$\pi/4$	**0.9**	0.258601

Table 3. Skin friction variations for isothermal temperature.

Pr	Gr	ωt	t	τ_{iso}
0.71	2	$\pi/4$	1.5	1.76398
7.0	2	$\pi/4$	1.5	1.96976
0.71	**4**	$\pi/4$	1.5	4.76402
0.71	2	$\boldsymbol{\pi/2}$	1.5	2.71942
0.71	2	$\pi/4$	**2.0**	2.30887

each Pr, Gr, ωt and t increases the ramped and isothermal skin frictions, τ_{ramp} and τ_{iso} at the surface. On the other hand, Nusselt number Nu is found to increase for large values of Pr and t for ramped wall temperature whereas the Nusselt number related to isothermal temperature increases with increasing Pr but decreases with increasing t.

Table 4. Nusselt's number variations for ramped wall temperature.

Pr	t	$\mathrm{Nu}_{\mathrm{ramp}}$
0.71	0.6	0.32634
7.0	0.6	1.02470
0.71	**0.9**	0.39908

Table 5. Nusselt's number variations for isothermal temperature.

Pr	t	$\mathrm{Nu}_{\mathrm{iso}}$
0.71	1.5	0.38815
7.0	1.5	1.21879
0.71	**2.0**	0.33615

9 Concluding remarks

An exact analysis is performed to study the unsteady convection flow of nanofluids bounded by an infinite vertical plate oscillating in its own plane. The fluid motion is induced due to free convection and bounding plate with ramped wall temperature. Closed form solutions for velocity and temperature are obtained using the Laplace transform technique. They satisfy the governing equations together with initial and boundary conditions and can be further used to verify the validity of other numerical solutions obtained for more complicated transient free convection flow of nanofluids. Both cases of ramped and isothermal plate temperatures are discussed. Corresponding expressions for the Nusselt number and skin friction are also evaluated for both ramped and isothermal plate conditions. Some special and limiting cases are also discussed. On the other hand, the present problem of natural convection flow of nanofluids over an infinite vertical flat plate has immediate applications in solar film collectors, heat exchangers technology, material sprocessing exploiting vertical surfaces, geothermal energy storage and all those processes which are highly affected by heat transfer concept. Amongst others, one of the technological applications of nanoparticles is the use of heat transfer fluids containing suspensions of nanoparticles to confront cooling problems in the thermal systems [28]. The following main results are concluded:

- An increase in nanoparticle volume fraction increases the nanofluid temperature, which leads to an increase in the heat transfer rates.
- Ramped velocity and temperature are smaller than isothermal velocity and temperature.
- Base fluid (water) has lower velocity whereas Al_2O_3 has maximum velocity.
- The surface skin friction increases for large values of Pr, Gr, ωt and t.
- Pr leads to an increase in the heat transfer rate.
- Silver water nanofuid is proven to have better heat transfer rate than the other three types of nanofluids.
- Skin-friction increases with increasing values of Pr, Gr, ωt and t for ramped wall temperature as well as isothermal temperature.
- The Nusselt number increases with increasing values of Pr and t for ramped wall temperature whereas Nusselt number associated with isothermal temperature increases with increasing Pr but decreases with increasing t.
- Our solutions are found identical to those obtained by Nandkeolyar *et al.* [37].

The authors would like to acknowledge the SBKWU (HEC), Pakistan, Ministry of Education Malaysia (MOE) and Research Management Centre-UTM for the financial support through vote numbers 06H67 and 4F255 for this research.

References

1. V. Rajesh, Int. J. Appl. Math. Mech. **6**, 1 (2010).
2. M. Narahari, Appl. Mech. Mater. **110**, 2228 (2012).
3. A.V. Kuznetsov, D.A. Nield, Int. J. Therm. Sci. **49**, 243 (2010).
4. M. Turkyilmazoglu, I. Pop, Int. J. Heat Mass Transfer **55**, 7635 (2012).
5. S. Sengupta, Int. J. Math. Arch. **2**, 1266 (2011).
6. S. Choi, Dev. Appl. Non-Newtonian Flows **66**, 99 (1995).
7. A.J. Chamkha, A.M. Rashad, Int. J. Numer. Methods Heat Fluid Flow **22**, 1073 (2012).
8. J.A. Eastman, S.U.S. Cho, S. Li, L.J. Thompson, S. Lee, in *Fall meeting of the Materials Research Society* (Boston, USA, 1997).
9. J.A. Eastman, S.U.S. Cho, S. Li, L.J.J. Metastable, Nano-Crystalline Mater. **2**, 629 (1998).
10. S.K. Das, N. Putra, W. Roetzel, Int. J. Heat Mass Transfer **46**, 851 (2003).
11. S.K. Das, N. Putra, W. Roetzel, Trans. ASME J. Heat Transfer **125**, 567 (2003).
12. J. Buongiorno, ASME J. Heat Transfer **128**, 240 (2006).
13. J. Buongiorno, D.C. Venerus, N. Prabhat, J. Appl. Phys. **106**, 094312 (2009).
14. S. Ahmed, I. Pop, Int. Commun. Heat Mass Transfer **37**, 987 (2010).
15. M.A.A. Hamad, I. Pop, A.I. Md. Ismail, Nonlinear Anal.: Real World Appl. **12**, 1338 (2011).
16. M.A.A. Hamad, Int. Commun. Heat Mass Transfer **38**, 487 (2011).
17. M. Qasim, I. Khan, S. Shafie, Math. Prob. Eng. **2013**, 254973 (2013).
18. N. Bachok, A. Ishak, I. Pop, Int. J. Therm. Sci. **49**, 1663 (2010).
19. R. Kandasamy, P. Loganathan, P.P. Arasu, Nucl. Eng. Des. **241**, 2053 (2011).
20. A. Mahdy, Nucl. Eng. Des. **249**, 248 (2012).
21. M.I. Anwar, I. Khan, S. Shafie, M.Z. Salleh, Int. J. Phys. Sci. **7**, 4081 (2012).
22. M.I. Anwar, I. Khan, M.Z. Salleh, A. Hasnain, S. Shafie, Wulfenia J. **19**, 367 (2012).
23. M.H. Yasi, N.M. Arifi, R. Nazar, F. Ismail, I. Pop, Adv. Sci. Lett. **13**, 833 (2012).
24. W. Ibrahim, O.D. Makinde, Comp. Fluids **86**, 433 (2013).
25. W.A. Khan, A. Aziz, Int. J. Therm. Sci. **50**, 2154 (2011).
26. M.J. Uddin, O.A. Bég, A.I.M. Ismail, Math. Prob. Eng. **2014**, 179172 (2014).
27. M.J. Uddin, W.A. Khan, N.S. Amin, PLoS ONE **9**, e99384 (2014).
28. P. Loganathan, P.N. Chand, P. Ganesan, *Radiation effects on an unsteady natural convective flow of a nanofluid past an infinite vertical plate*, Vol. **8** (World Scientific Publishing Company, 2013) pp. 1350001–1350010.
29. M. Turkyilmazoglu, J. Heat Transfer **136**, 031704 (2014).
30. A.A. Hayday, D.A. Bowlus, R.A. Mc Graw, ASME J. Heat Transfer **89**, 244 (1967).
31. M. Kelleher, ASME J. Heat Transfer **93**, 349 (1971).
32. T.T. Kao, Lett. Heat Mass Transfer **2**, 419 (1975).
33. J.A. Schetz, R. Eichhorn, Trans. ASME **61**, 334 (1962).
34. P. Chandran, N.C. Sacheti, A.K. Singh, Heat Mass Transfer **41**, 459 (2005).
35. G.S. Seth, MdS. Ansari, R. Nandkeolyar, Heat Mass Transfer **47**, 551 (2011).
36. M. Narahari, OA Beg, AIP Conf. Ser. **1225**, 743 (2010).
37. R. Nandkeolyar, M. Das, H. Pattnayak, J. Orissa Math. Soc. **32**, 15 (2013).
38. Samiulhaq, I. Khan I, F. Ali, S. Shafie, J. Phys. Soc. Jpn. **81**, 4401 (2012).
39. Samiulhaq, S. Ahmed, D. Vieru, I. Khan, S. Shafie, Plos One **5**, e88766 (2014).
40. Z. Ismail, A. Hussanan, I. Khan, S. Shafie, Int. J. Appl. Math. Stat. **45**, 77 (2013).